Supplemental Data

A

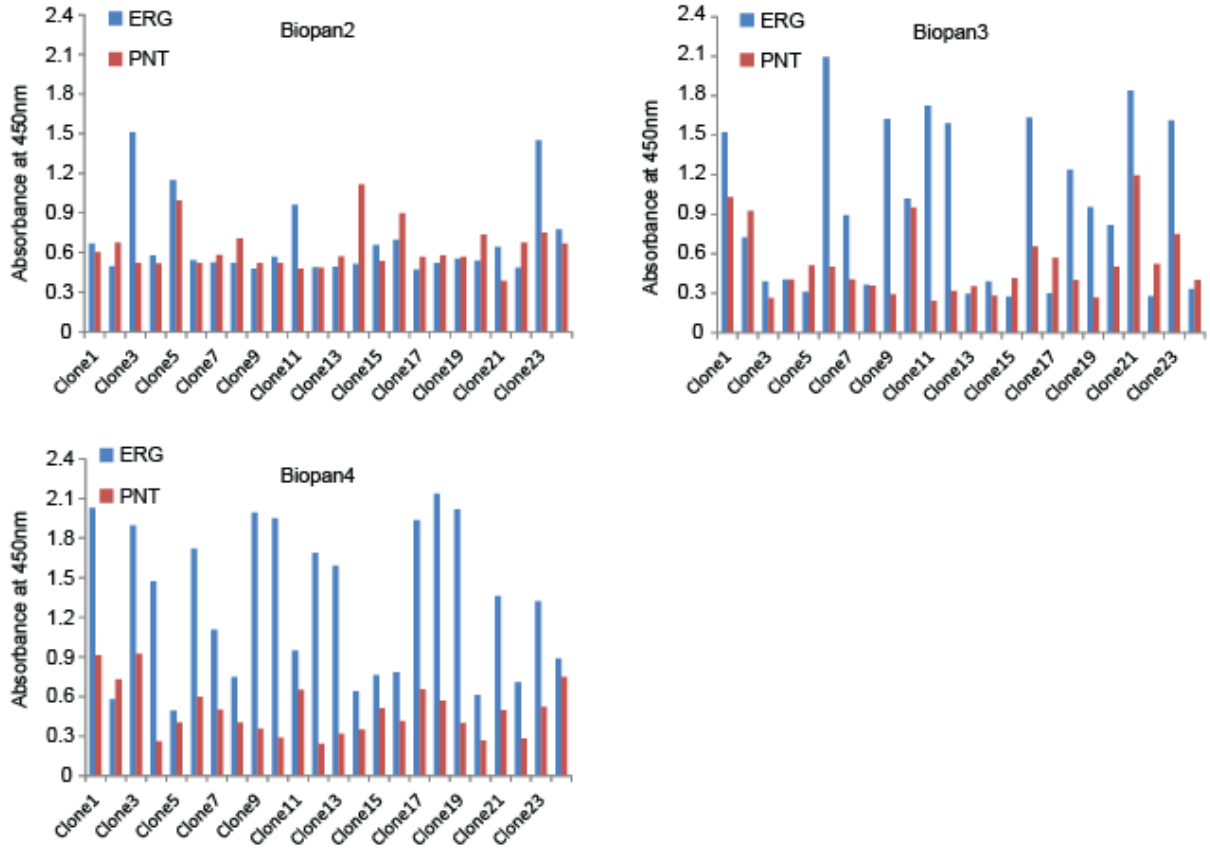

B

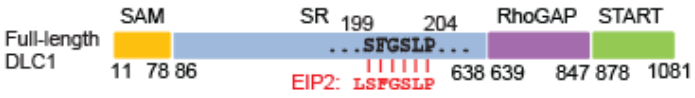

C

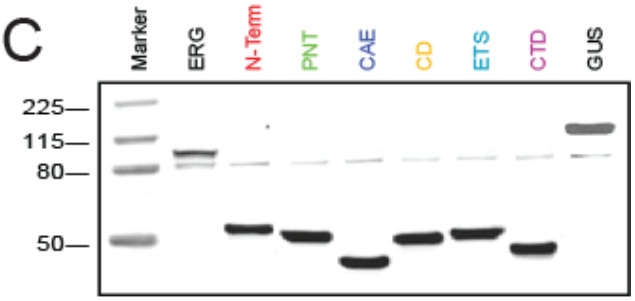

D

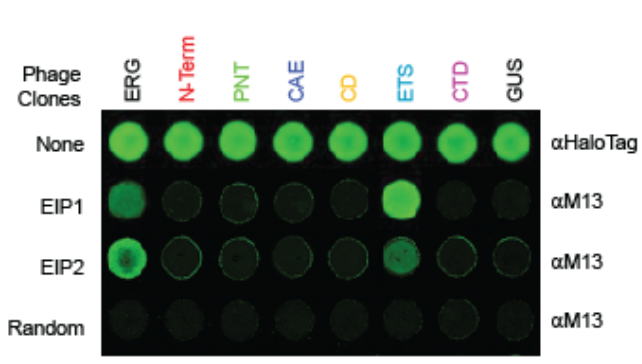

E

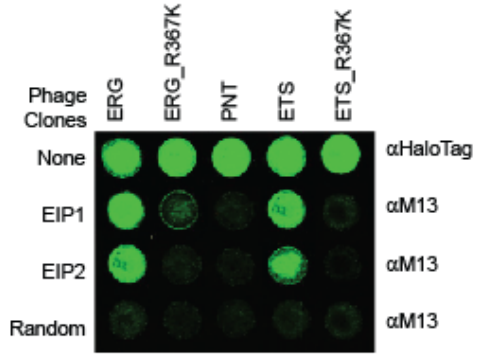

Figure S1. C**haracterization of ERG binding peptides, related to Figure 1.**
(**A**) Validation of randomly selected ERG binding phage clones from the 2nd, 3rd and 4th enrichment using ELISA. ELISA plates were coated with either recombinant full-length ERG protein or PNT domain protein as negative control.
(**B**) Schematic representation of the domain structure of the DLC1 protein. Numbers indicate amino acid residue and functional domains are indicated as: SAM, N-terminal α motif (11-78), SR, serine-rich region (86-638), RhoGAP, Rho-GAP domain (639-847), START, C-terminal steroidogenic acute regulatory protein related lipid-transfer domain (878-1081). The alignment between the EIP2 sequence and the SR domain of DLC1 (199-204) is depicted.
(**C**) Western blot analysis of halo-fusion ERG proteins, ETS sub-domains and GUS control expressed by SP6 High-Yield Wheat Germ lysate.
(**D, E**) Representative protein array image showing the interaction between phage peptides and ERG protein or its domains. Respective halo-tagged ERG and the domains (**D**), or ERG and its mutants (**E**) were immobilized on a protein array surface as a matrix with each column representing different proteins. The 1st row shows equal amounts of recombinant proteins detected by anti-halo antibody. The 2nd to 4th rows represent ERG-binding phages (EIP1 or EIP2) or random phage incubated with each recombinant protein and detected by anti-M13 antibody.

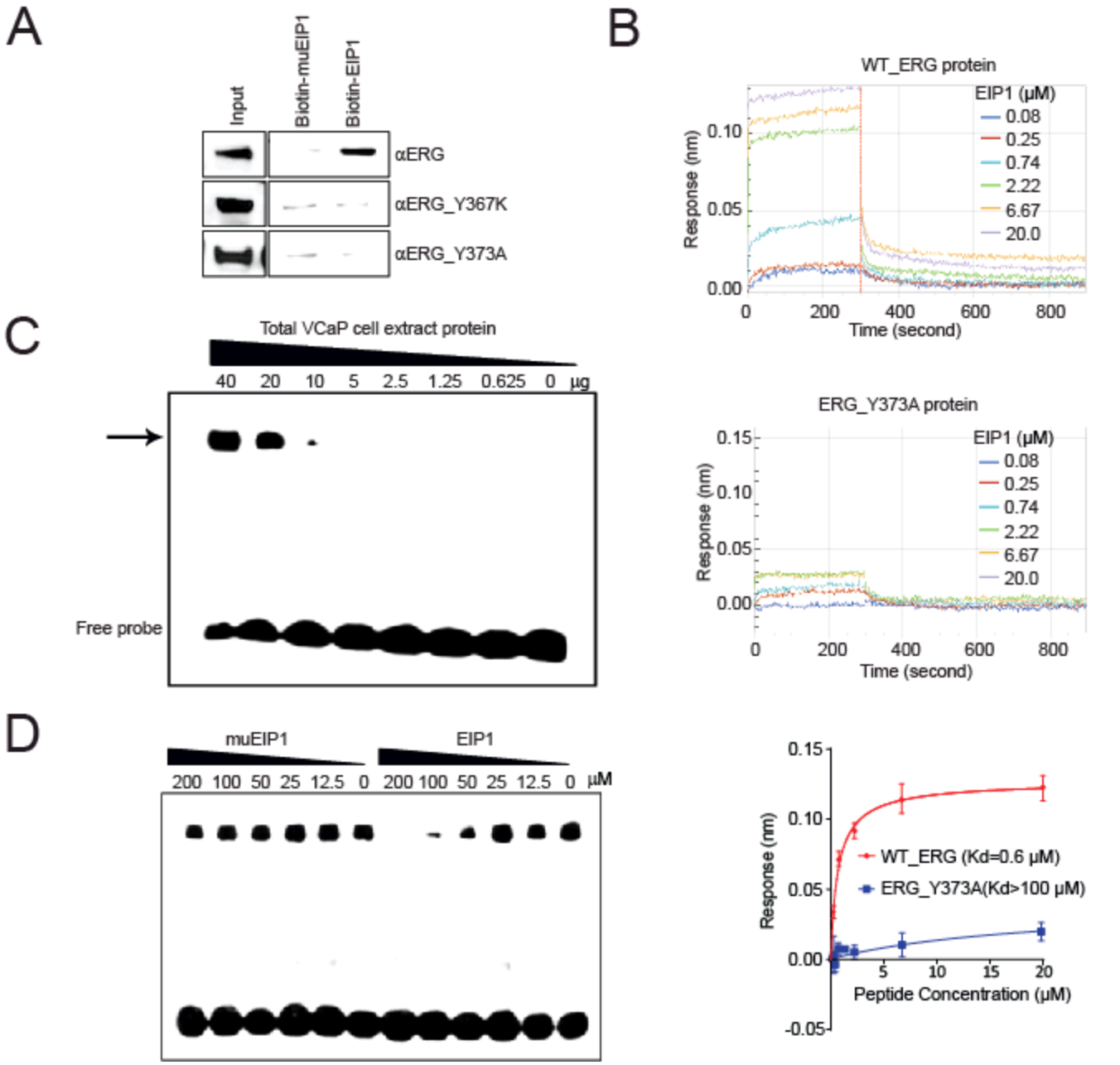

Figure S2. **Binding properties of synthetic peptides, related to Figure 2.**
(**A**) Pull-down experiment was performed by incubating purified recombinant proteins and biotin-peptides. Eluates from the pull-downs were subjected to immunoblot analysis using an anti-ERG antibody.
(**B**) Representative sensorgrams and steady-state analysis for both WT_ERG and ERG_Y373A binding to EIP1. Real-time binding was measured by immobilization of biotinylated proteins to the streptavidin biosensors and subsequent interactions with varying concentrations of synthetic peptides as indicated. Steady-state analysis plots show the response versus peptide concentration curves derived from the raw binding data. Dissociation constants (Kd) represent the peptide concentration yielding half-maximal binding to the protein. The experiments mean ± SEM is shown.
(**C**) Electrophoretic mobility shift assay (EMSA) for ERG and ETS binding sequence (EBS). VCaP cell extract at different amount was incubated with biotin conjugated EBS, then subjected to a non-denatured gel electrophoresis. Arrow indicates migration of DNA-binding complexes.
(**D**) Competitive EMSA demonstrates that EIP1 disrupts the interaction of ERG with DNA.

TABLE S1. Binding affinity of the synthetic peptides determined by OctetRED, relate to Figure 2.
N.D.: not determined.

Synthetic peptides	Name	Kd (μM)
LPPYLFT	EIP1	0.6
FSASSPA		21.1
FSFGSLP		2.1
LSFGSLP	EIP2	1.8
LAFGSLP		6.4
FTFGSLP		3.9
LTFGSLP		2.9
MTFGTLP		4.6
YTFGTLP		3.2
LRFGTLP		7.9
LSFGSFP		12.5
LSFGTFP		9.2
LPPALFT	muEIP1	N.D.
LSAGSAP	muEIP2	N.D.
LPPTFLY	Scr	N.D.

A

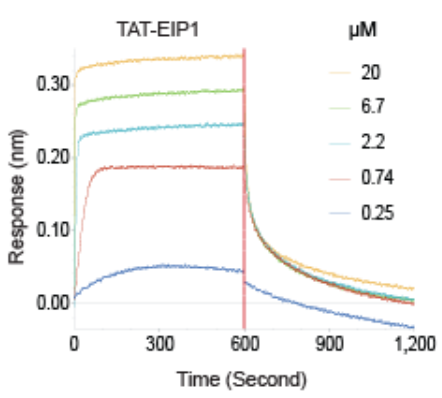
TAT-EIP1
μM
20
6.7
2.2
0.74
0.25
Response (nm)
0.30
0.20
0.10
0.00
0
300
600
900
1,200
Time (Second)

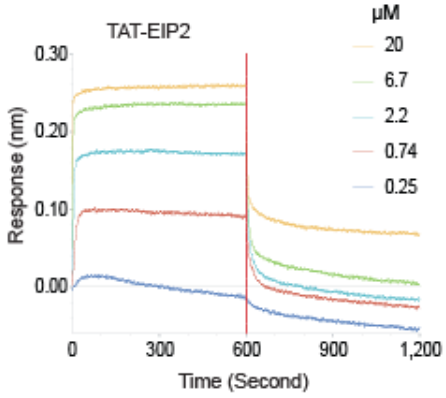
TAT-EIP2
μM
20
6.7
2.2
0.74
0.25
Response (nm)
0.30
0.20
0.10
0.00
0
300
600
900
1,200
Time (Second)

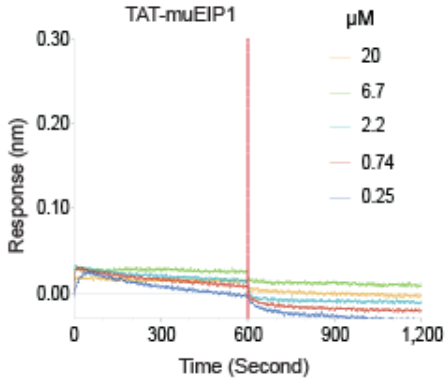
TAT-muEIP1
μM
20
6.7
2.2
0.74
0.25
Response (nm)
0.30
0.20
0.10
0.00
0
300
600
900
1,200
Time (Second)

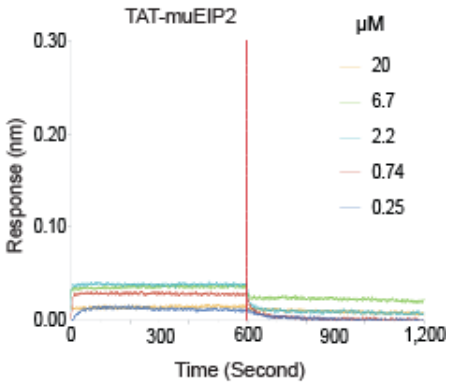
TAT-muEIP2
μM
20
6.7
2.2
0.74
0.25
Response (nm)
0.30
0.20
0.10
0.00
0
300
600
900
1,200
Time (Second)

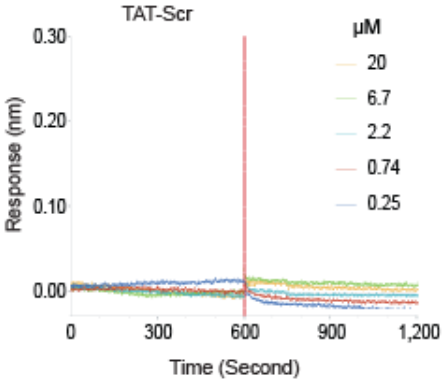
TAT-Scr
μM
20
6.7
2.2
0.74
0.25
Response (nm)
0.30
0.20
0.10
0.00
0
300
600
900
1,200
Time (Second)

B

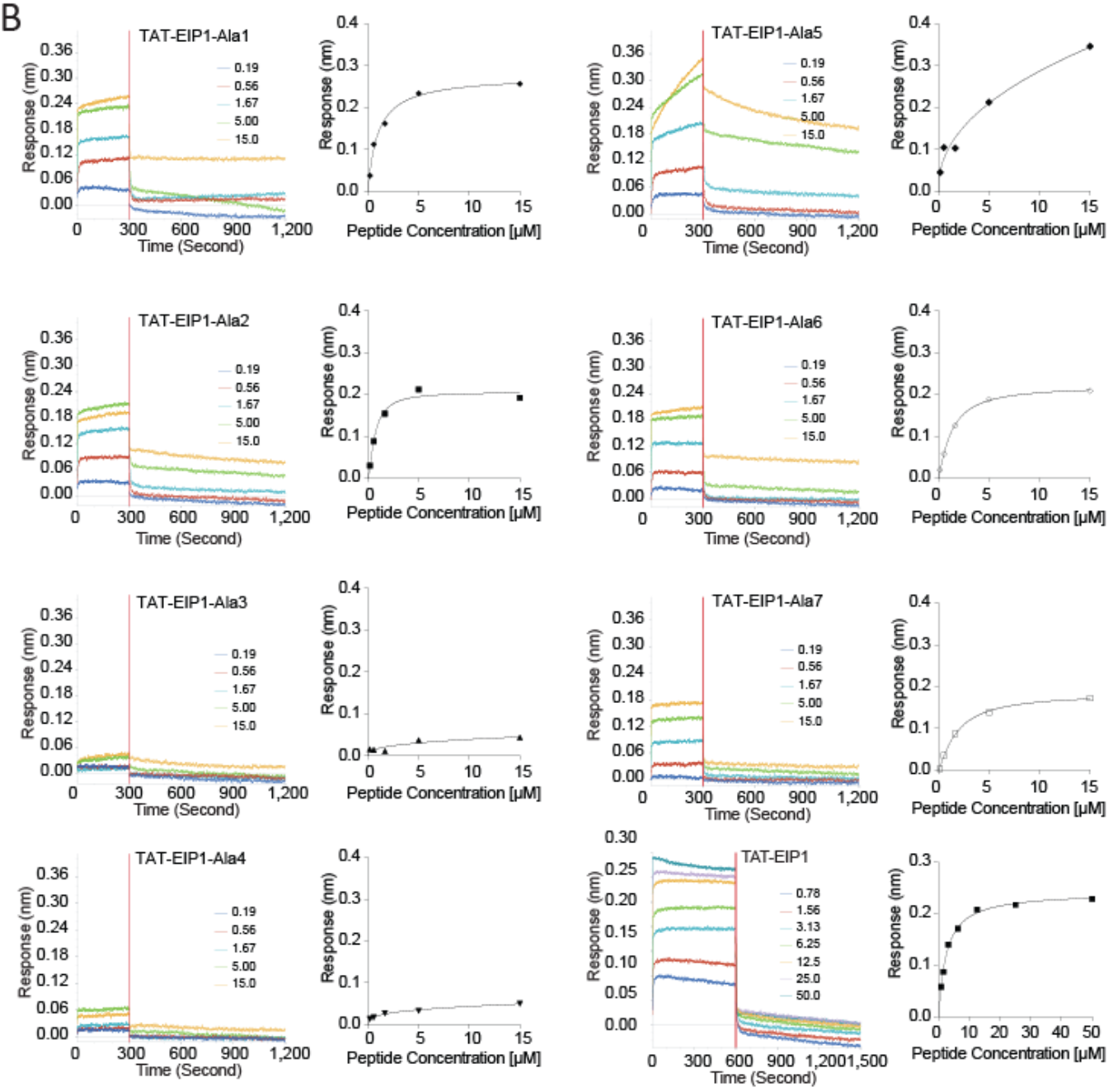

C

Name	Peptide Sequences	Kd (μM)
TAT-EIP1	LPPYLFTGGRKKRRQRRRG	1.07
TAT-EIP1-Ala1	APPYLFTGGRKKRRQRRRG	1.13
TAT-EIP1-Ala2	LAPYLFTGGRKKRRQRRRG	0.88
TAT-EIP1-Ala3	LPAYLFTGGRKKRRQRRRG	>100
TAT-EIP1-Ala4	LPPALFTGGRKKRRQRRRG	>100
TAT-EIP1-Ala5	LPPYAFTGGRKKRRQRRRG	Non-specific
TAT-EIP1-Ala6	LPPYLATGGRKKRRQRRRG	1.29
TAT-EIP1-Ala7	LPPYLFAGGRKKRRQRRRG	1.86

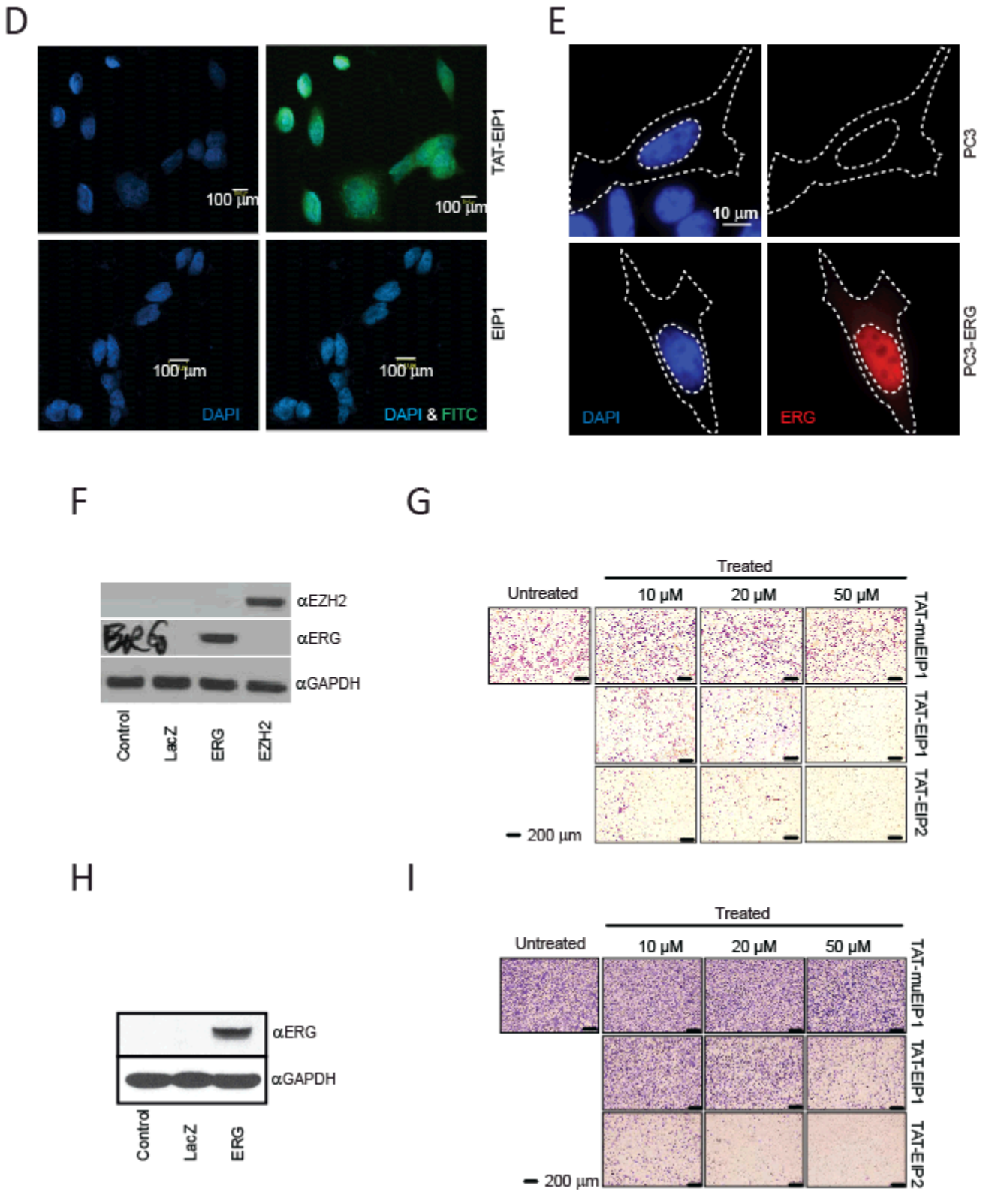
D
100 µm
100 µm
TAT-EIP1
100 µm
100 µm
EIP1
DAPI
DAPI & FITC
E
10 µm
PC3
PC3-ERG
DAPI
ERG
F
αEZH2
αERG
αGAPDH
Control
LacZ
ERG
EZH2
G
Treated
Untreated
10 µM
20 µM
50 µM
TAT-muEIP1
TAT-EIP1
TAT-EIP2
200 µm
H
αERG
αGAPDH
Control
LacZ
ERG
I
Treated
Untreated
10 µM
20 µM
50 µM
TAT-muEIP1
TAT-EIP1
TAT-EIP2
200 µm

Figure S3. Cell-permeable peptides block ERG-mediated cell invasion, related to Figure 3.
(**A**) Representative OctetRED sensorgrams for ERG binding to cell permeable peptides or controls. The real-time binding was measured as in **Figure 2B.**
(**B**) Representative OctetRED sensorgrams for the mutant TAT-EIP1. The real-time binding was measured as in **Figure 2B**.
(**C**) Kinetic binding data for the mutant TAT-EIP1.
(**D**) VCaP cells were treated with FITC-labeled TAT-EIP1 or EIP1, mounted and counterstained with DAPI before imaging. Scale bar: 10 μm.
(**E**) Representative pseudocolored images of PC3 (top) and PC3 cells over-expressing ERG (bottom). Cells were stained with ERG antibody (red) and the nuclei were stained with DAPI (blue). Nuclear and cell boundaries are depicted with white dotted line. Scale bar, 5 μm.
(**F**) Western blot analysis to determine expression levels of ERG and EZH2 in the stable isogenic RWPE-1 models.
(**G**) Invasion assays of RWPE1-ERG cells in the presence of TAT-EIPs and mutant EIP1. The cells were treated with the peptide inhibitors as indicated for 24 hours and then incubated another 48 hours before fixation and imaging.
(**H**) Western blot analysis of ERG expression in stable isogenic PC3 cells.
(**I**) Invasion assays of PC3-ERG cells performed as in **Figure 3E-H**.

A

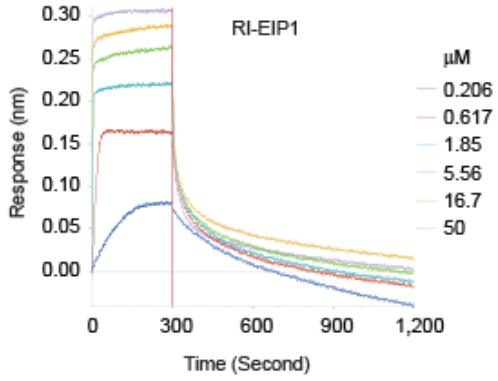
RI-EIP1
Response (nm)
0.30
0.25
0.20
0.15
0.10
0.05
0.00
0
300
600
900
1,200
Time (Second)
µM
0.206
0.617
1.85
5.56
16.7
50

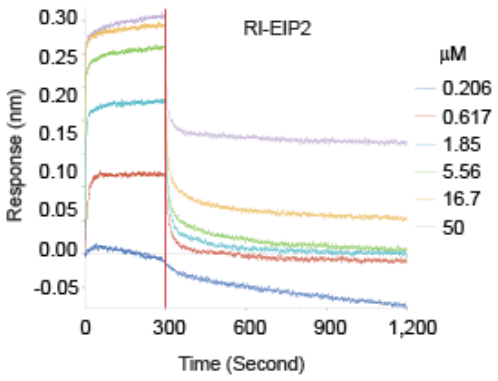
RI-EIP2
Response (nm)
0.30
0.25
0.20
0.15
0.10
0.05
0.00
-0.05
0
300
600
900
1,200
Time (Second)
µM
0.206
0.617
1.85
5.56
16.7
50

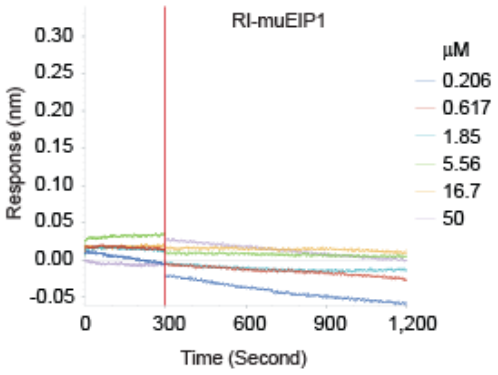
RI-muEIP1
Response (nm)
0.30
0.25
0.20
0.15
0.10
0.05
0.00
-0.05
0
300
600
900
1,200
Time (Second)
µM
0.206
0.617
1.85
5.56
16.7
50

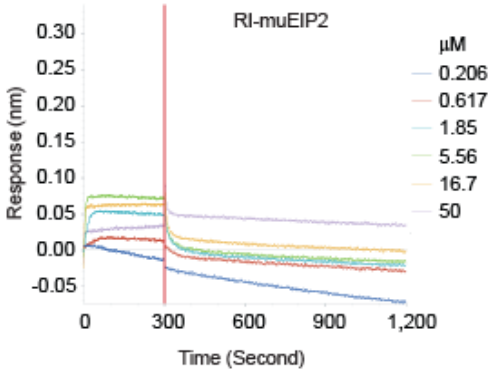
RI-muEIP2
Response (nm)
0.30
0.25
0.20
0.15
0.10
0.05
0.00
-0.05
0
300
600
900
1,200
Time (Second)
µM
0.206
0.617
1.85
5.56
16.7
50

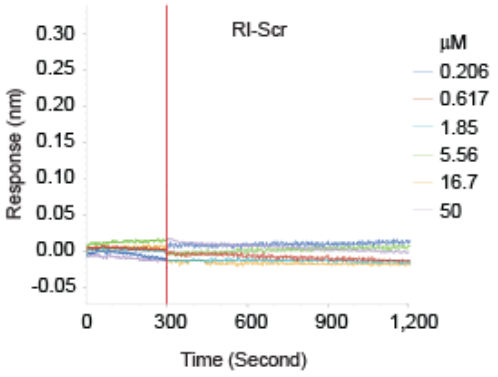
RI-Scr
Response (nm)
0.30
0.25
0.20
0.15
0.10
0.05
0.00
-0.05
0
300
600
900
1,200
Time (Second)
µM
0.206
0.617
1.85
5.56
16.7
50

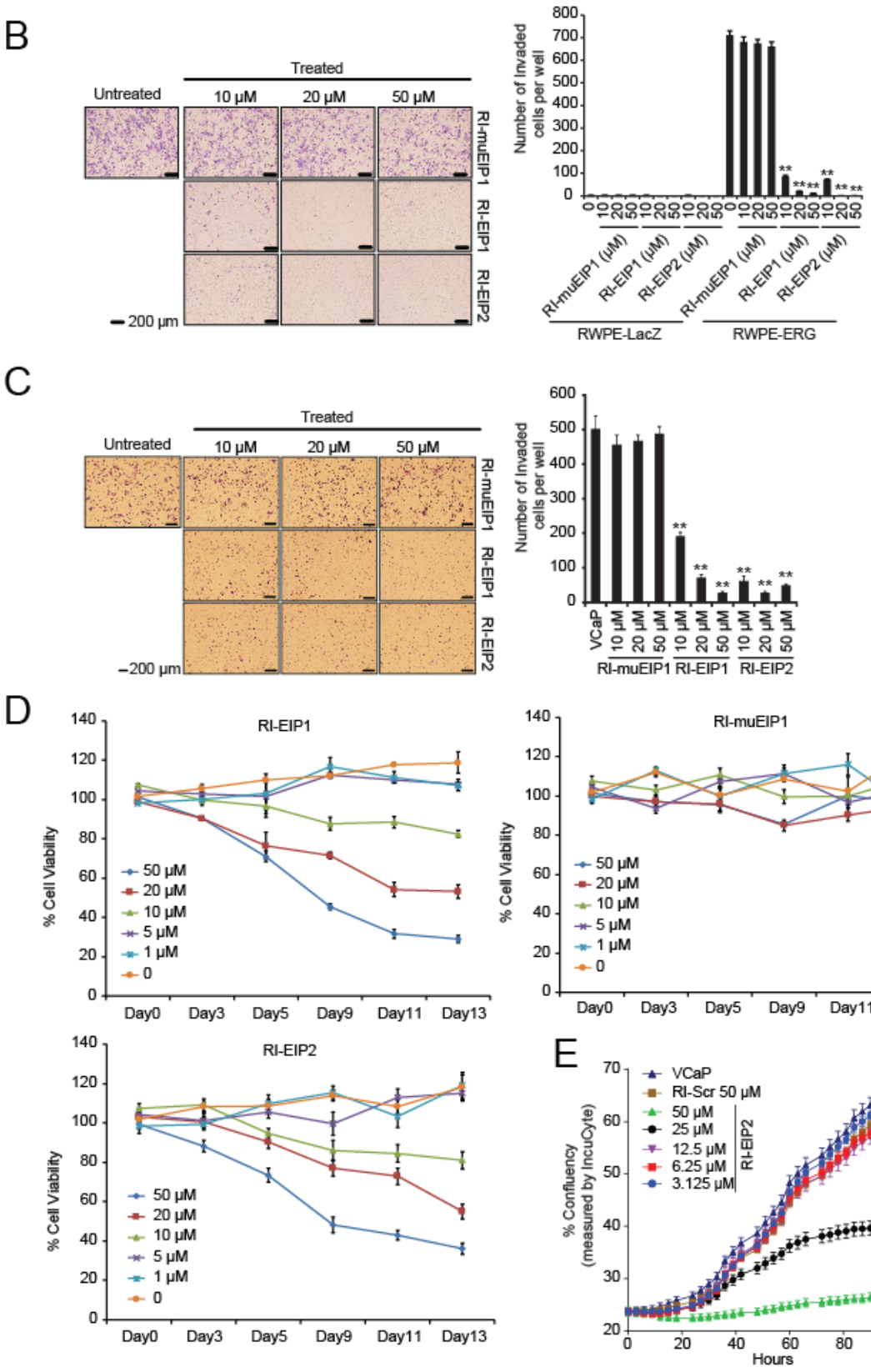
B
Treated
Untreated
10 μM
20 μM
50 μM
RI-muEIP1
RI-EIP1
RI-EIP2
200 μm
Number of Invaded cells per well
RI-muEIP1 (μM)
RI-EIP1 (μM)
RI-EIP2 (μM)
RWPE-LacZ
RWPE-ERG
C
VCaP
RI-muEIP1
RI-EIP1
RI-EIP2
D
RI-EIP1
RI-muEIP1
RI-EIP2
% Cell Viability
50 μM
20 μM
10 μM
5 μM
1 μM
0
Day0
Day3
Day5
Day9
Day11
Day13
E
VCaP
RI-Scr 50 μM
50 μM
25 μM
12.5 μM
6.25 μM
3.125 μM
RI-EIP2
% Confluency (measured by IncuCyte)
Hours

F

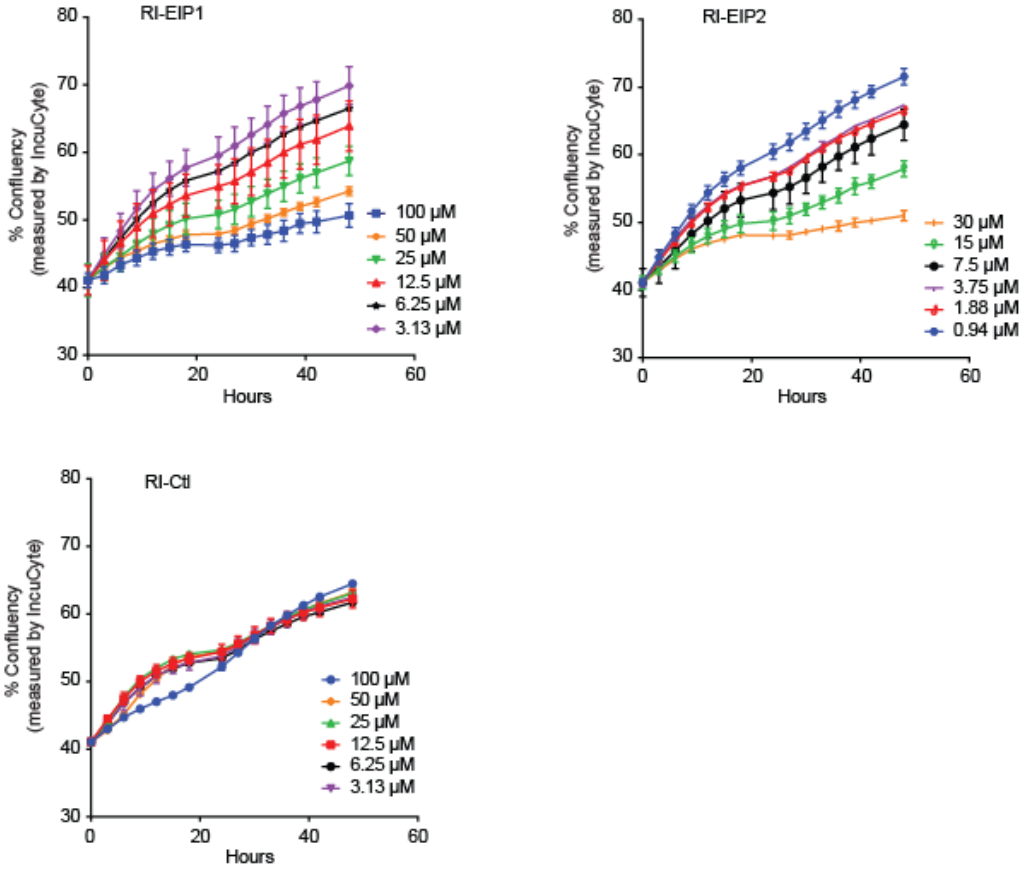
RI-EIP1
% Confluency (measured by IncuCyte)
Hours
100 µM
50 µM
25 µM
12.5 µM
6.25 µM
3.13 µM
RI-EIP2
30 µM
15 µM
7.5 µM
3.75 µM
1.88 µM
0.94 µM
RI-Ctl

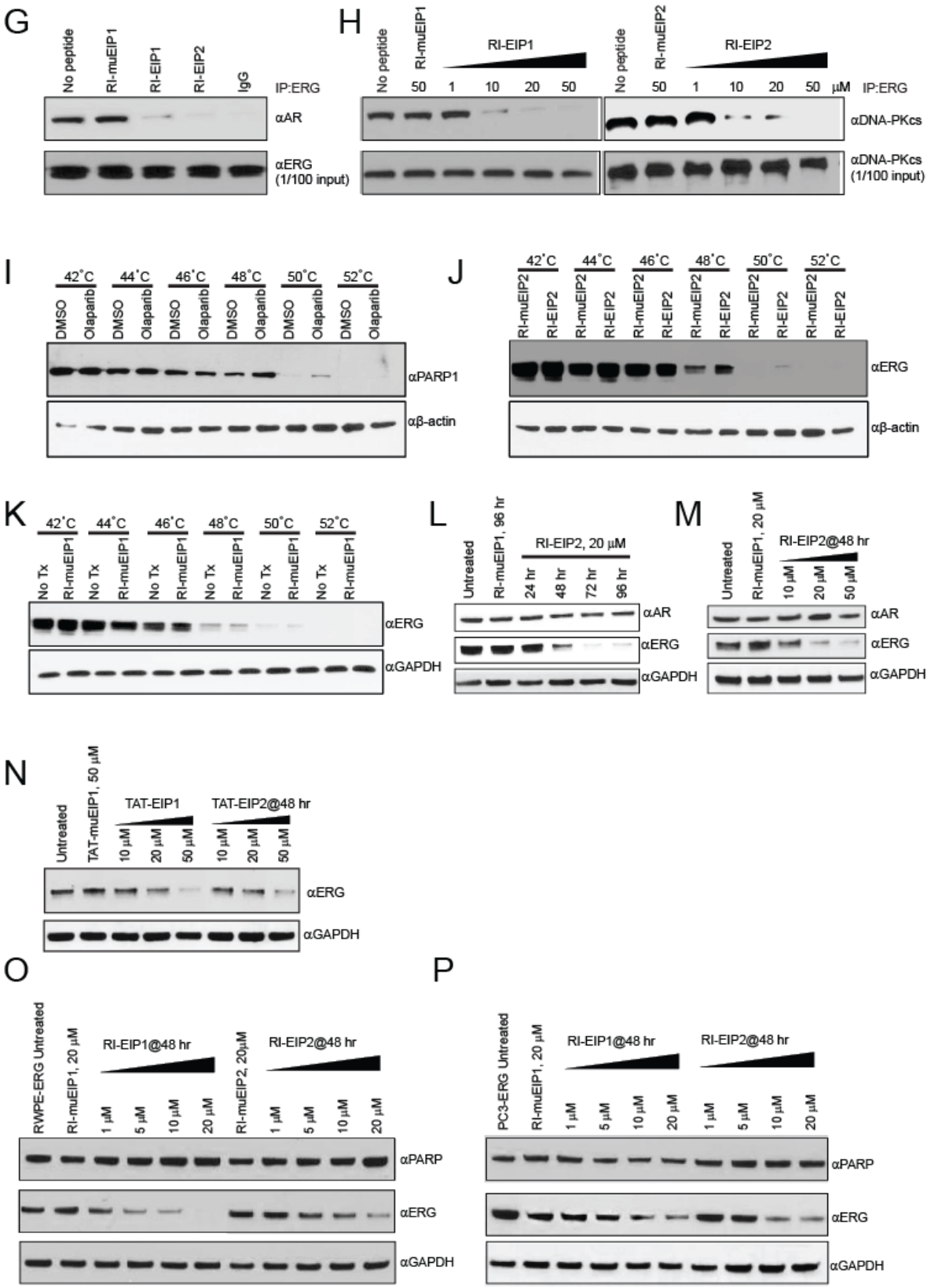
G
No peptide
RI-muEIP1
RI-EIP1
RI-EIP2
IgG
IP:ERG
αAR
αERG (1/100 input)
H
No peptide
RI-muEIP1
RI-EIP1
50 1 10 20 50
No peptide
RI-muEIP2
RI-EIP2
50 1 10 20 50 μM
IP:ERG
αDNA-PKcs
αDNA-PKcs (1/100 input)
I
42˚C 44˚C 46˚C 48˚C 50˚C 52˚C
DMSO Olaparib
αPARP1
αβ-actin
J
42˚C 44˚C 46˚C 48˚C 50˚C 52˚C
RI-muEIP2 RI-EIP2
αERG
αβ-actin
K
42˚C 44˚C 46˚C 48˚C 50˚C 52˚C
No Tx RI-muEIP1
αERG
αGAPDH
L
Untreated
RI-muEIP1, 96 hr
RI-EIP2, 20 μM
24 hr 48 hr 72 hr 96 hr
αAR
αERG
αGAPDH
M
Untreated
RI-muEIP1, 20 μM
RI-EIP2@48 hr
10 μM 20 μM 50 μM
αAR
αERG
αGAPDH
N
Untreated
TAT-muEIP1, 50 μM
TAT-EIP1
TAT-EIP2@48 hr
10 μM 20 μM 50 μM 10 μM 20 μM 50 μM
αERG
αGAPDH
O
RWPE-ERG Untreated
RI-muEIP1, 20 μM
RI-EIP1@48 hr
1 μM 5 μM 10 μM 20 μM
RI-muEIP2, 20μM
RI-EIP2@48 hr
1 μM 5 μM 10 μM 20 μM
αPARP
αERG
αGAPDH
P
PC3-ERG Untreated
RI-muEIP1, 20 μM
RI-EIP1@48 hr
1 μM 5 μM 10 μM 20 μM
RI-EIP2@48 hr
1 μM 5 μM 10 μM 20 μM
αPARP
αERG
αGAPDH

Figure S4. Retroinverso EIPs specifically bind to and destabilize the ERG target, related to Figure 4.
(**A**) Representative OctetRED sensorgrams for ERG binding to retroinverso peptides. The real-time binding was measured as in **Figure 2B**.
(**B**) Boyden chamber transwell invasion assays of RWPE-ERG or LacZ cells performed as in **Figure 3E-H.** The data shown are the mean of three independent experiments.
(**C**) Boyden chamber transwell invasion assays of VCaP cells performed as in **Figure 3E-H.** The data shown are the mean of three independent experiments.
(**D**) VCaP cell proliferation measured by CellTiter-Glo after long-term treatment with RI-EIP2 (5 to 13 days as indicated). Luminescent signals were normalized to those of untreated VCaP cells. The data shown are the mean of three independent experiments.
(**E**) Confluence rate for VCaP cells measured as in **Figure 4C** except using RI-EIP2.
(**F**) Confluence rate for VCaP cells measured as in **Figure 4C** except the cells were cultured in charcoal stripped media.
(**G, H**) IP-Western blot analysis of AR (**G**) or DNA-PKcs (**H**) in VCaP cells treated with either RI-EIPs or -muEIPs. Cell lysates (1/100 IP input) were used as positive control. The assays were performed as in **Figure 3D**.
(**I**) Olaparib-treated VCaP cells were analyzed following temperature shift from 42°C to the indicated temperatures. PARP1 protein expression in the soluble fraction of the cell lysates was detected by Western blotting.
(**J, K**) VCaP cells were treated with either RI-EIP2 or RI-muEIP2 (**J**), or RI-muEIP1 or untreated (**K**). The CETSAs were performed as in **Figure 4F**.
(**L, M**) Immunoblot analysis of ERG, AR and GAPDH in VCaP cells treated with RI-EIP2 or RI-muEIP1 with 20 μM at indicated time points (**L**) or for 48 hr at indicated concentrations (**M**). The assays were performed as in **Figure 4H-I**.
(**N**) Immunoblot analysis of ERG and GAPDH in VCaP cells treated with TAT-EIPs or control peptides. The assays were performed as in **Figure 4H-I**.
(**O, P**) Immunoblot analysis of ERG, PARP and GAPDH in RWPE1-ERG (**O**) or PC3-ERG (**P**) treated with RI-EIPs or control peptides. The assays were performed as in **Figure 4H-I**.
For all experiments, mean ± SEM is shown. **, $p < 0.05$.

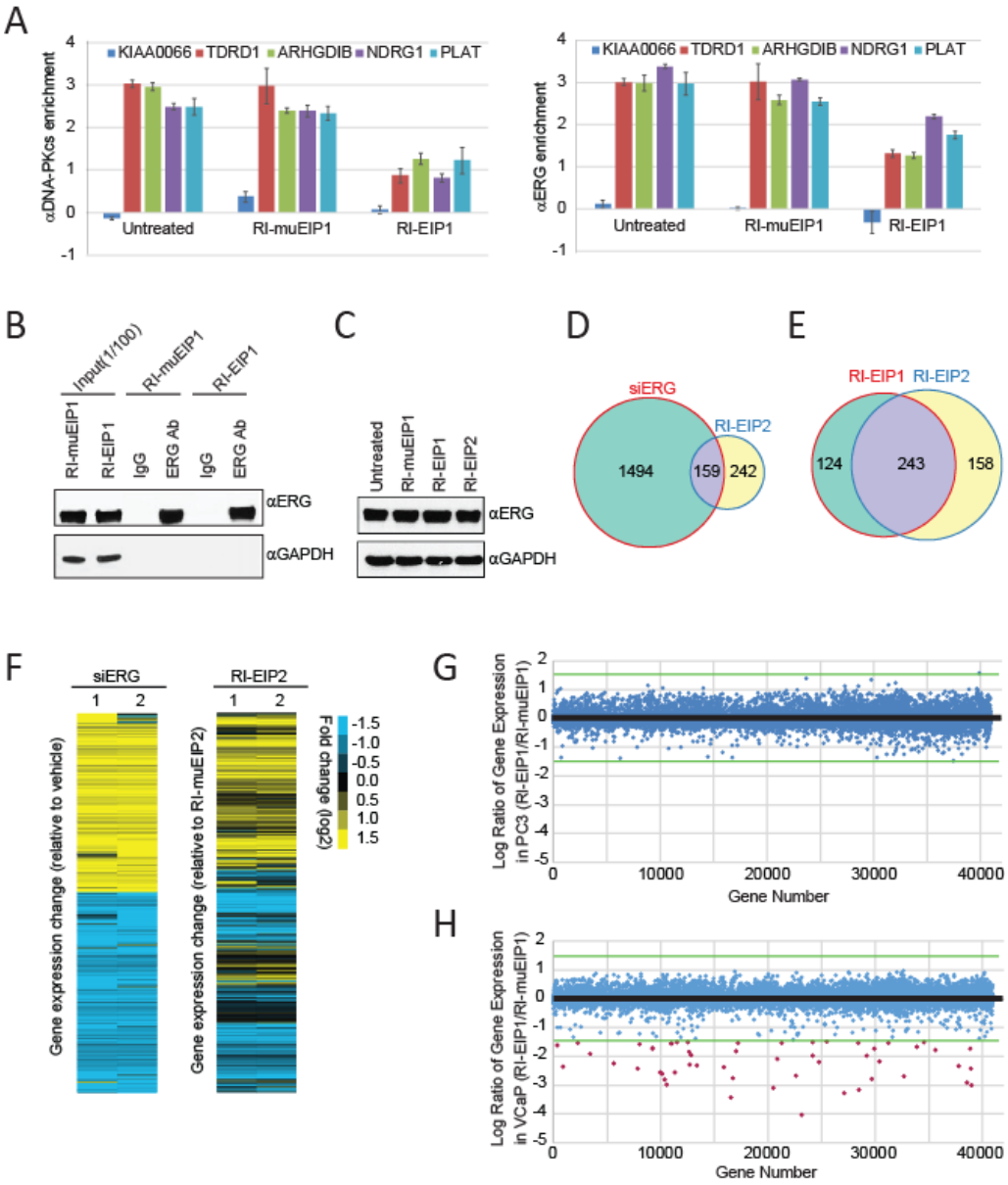

Figure S5. RI-EIPs disrupt ERG transcriptional activity, related to Figure 5.

(**A**) ChIP assays performed using ERG and DNA-PKcs antibodies on VCaP cells treated with the peptides for 12 hours prior to crosslinking. Q-PCRs were performed for several ERG-regulated genomic loci. KIAA0066 served as negative control gene. For all experiments, mean ± SEM is shown.

(**B**) Immunoblot analysis of ERG and GAPDH in the ChIP-seq samples precipitated by ERG antibody from the VCaP cell lysate in **Figure 5A**.

(**C**) Immunoblot analysis of ERG and GAPDH in VCaP cell treated by the indicated peptides for 12 hours. The total RNA extracted from the cells were used for gene expression assay in **Figure 5D-E.**

(**D**) Venn diagram illustrating the overlap of disregulated genes (greater than 2-fold, FDR<0.01) between siERG- and RI-EIP2-treated VCaP cells.

(**E**) Venn diagram illustrating the overlap of disregulated genes between RI-EIP1 and RI-EIP2-treated VCaP cells.

(**F**) Heatmap from microarray analysis of ERG knockdown by siERG or RI-EIP2 treatment in VCaP cells, comparing gene expression changes upon siERG knockdown and RI-EIP2 treatment.

(**G-H**) Scatter plots of gene expression, comparing the gene profiles in PC3 (**G**) or VCaP (**H**). Green lines indicate the cutoff of ±1.5; red spots highlight the downregulated genes with log2[ratio] < -1.5.

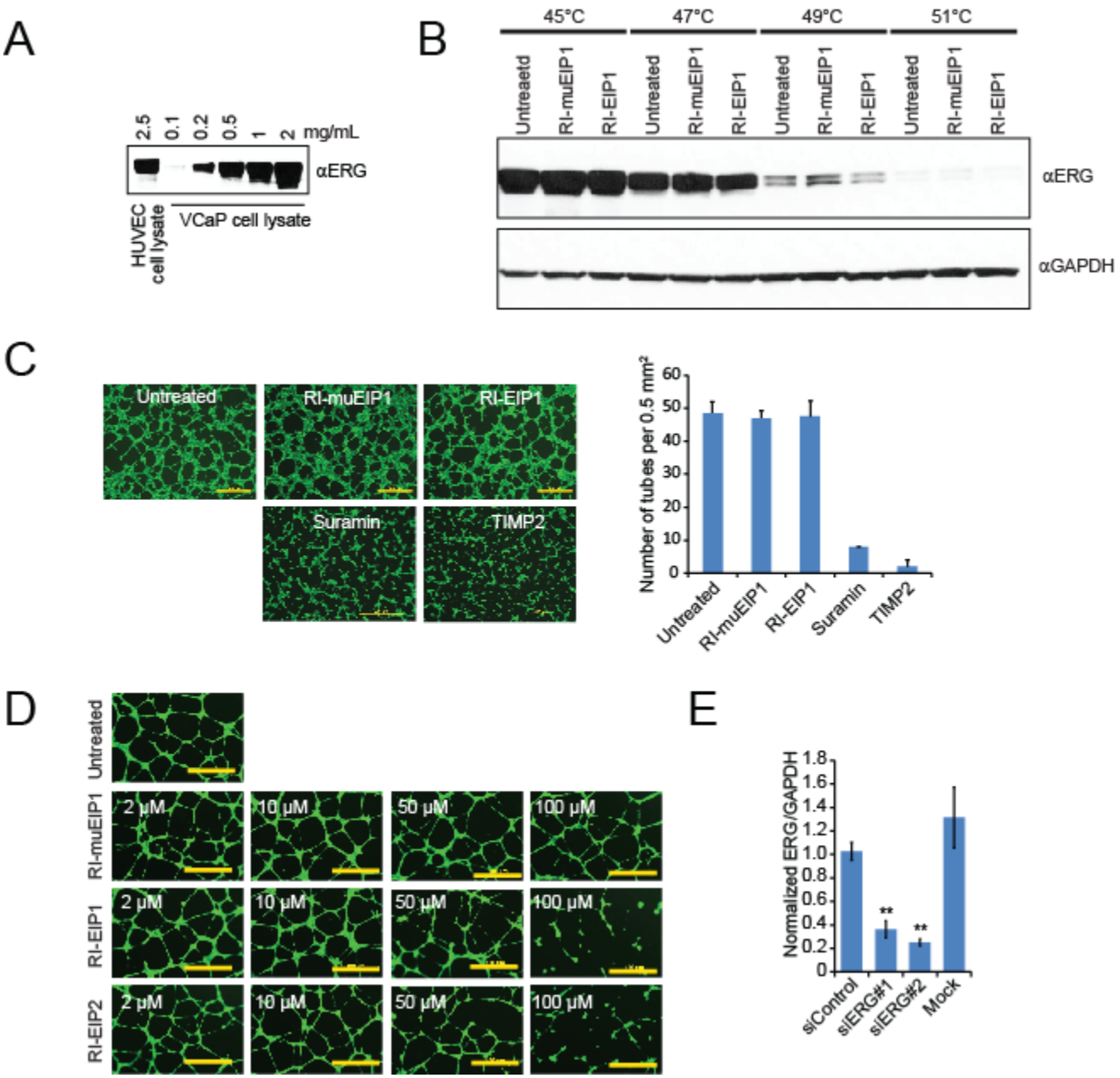

Figure S6. RI-EIPS have no effects on ERG-mediated angiogenesis, related to Figure 6.

(**A**) Relative ERG levels in HUVEC and VCaP cell lysates as evaluated by immunoblot analysis.

(**B**) The soluble ERG protein was measured by cellular thermal shift assay (CETSA) in HUVEC cells treated with 25 μM RI-EIP1 as performed in **Figure 4F**.

(**C**) Representative microphotographs of a 3D culture of mouse endothelial cells (MS1 with high mERG expression) (scale bar, 200 μm) in the presence of inhibitors as indicated. The bar graphs show the number of tubes/area of cells treated as indicated and analyzed by ImageJ software. The average lengths were calculated for each transductant from microphotographs captured in duplicate experiments performed.

(**D**) The phenotypic effect of RI-EIPs on vascular remodeling was tested in vitro using the Matrigel tube formation assay as in (**C**) in the presence of varying amount of RI-peptides. Scale bar: 100 μm.

(**E**) Q-PCR analysis of ERG mRNA levels in siERG HUVEC. The y-axis represents normalized mRNA expression level relative to GAPDH internal control.

Error bars represent ± SEM. **p value < 0.05.

A

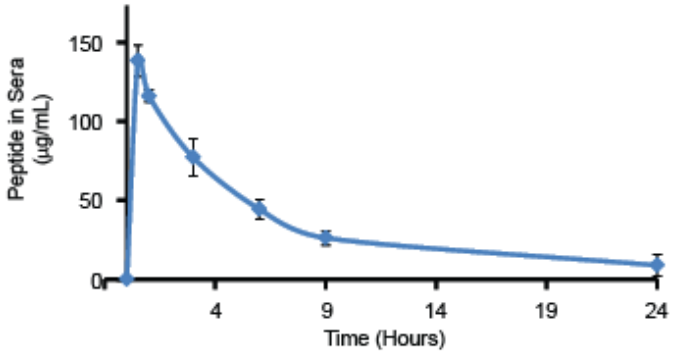
Peptide in Sera (μg/mL)
150
100
50
0
4
9
14
19
24
Time (Hours)

B

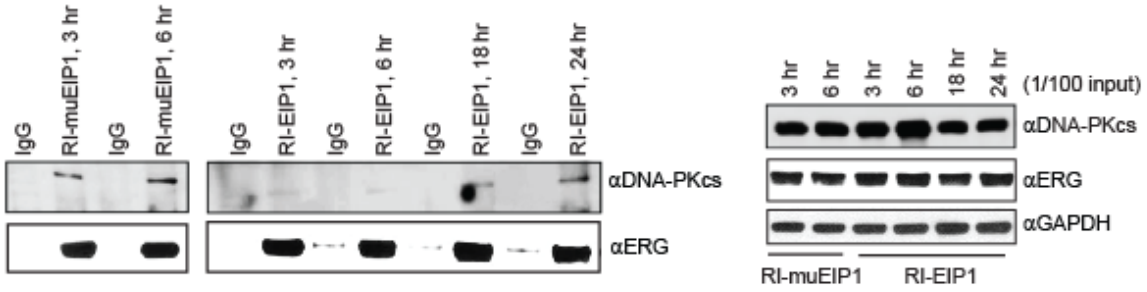
IgG
RI-muEIP1, 3 hr
IgG
RI-muEIP1, 6 hr
IgG
RI-EIP1, 3 hr
IgG
RI-EIP1, 6 hr
IgG
RI-EIP1, 18 hr
IgG
RI-EIP1, 24 hr
αDNA-PKcs
αERG
3 hr
6 hr
3 hr
6 hr
18 hr
24 hr
(1/100 input)
αDNA-PKcs
αERG
αGAPDH
RI-muEIP1
RI-EIP1

C

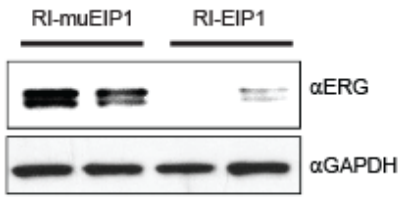
RI-muEIP1
RI-EIP1
αERG
αGAPDH

D

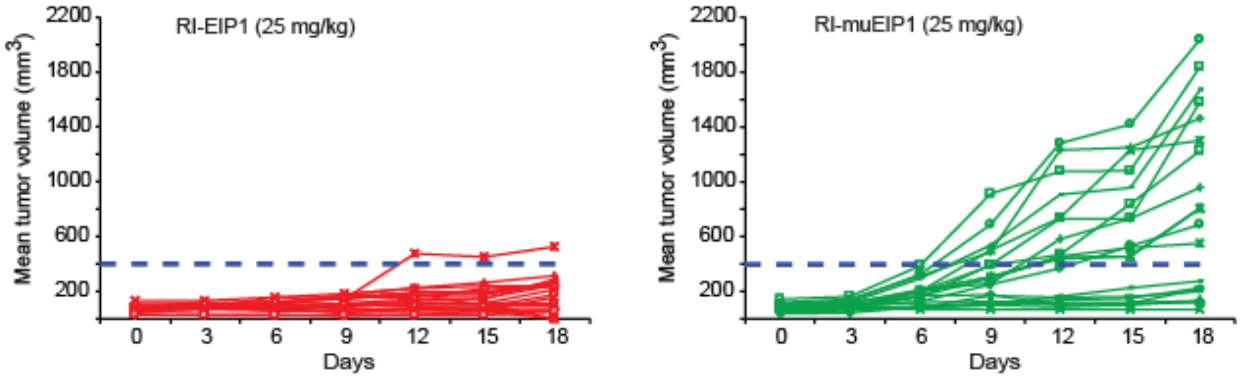
RI-EIP1 (25 mg/kg)
Mean tumor volume (mm3)
2200
1800
1400
1000
600
200
0
3
6
9
12
15
18
Days
RI-muEIP1 (25 mg/kg)
Mean tumor volume (mm3)
2200
1800
1400
1000
600
200
0
3
6
9
12
15
18
Days

E

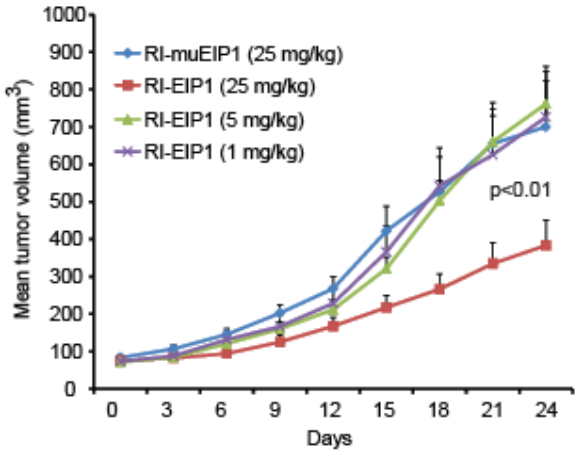
RI-muEIP1 (25 mg/kg)
RI-EIP1 (25 mg/kg)
RI-EIP1 (5 mg/kg)
RI-EIP1 (1 mg/kg)
p<0.01
Mean tumor volume (mm3)
Days

F

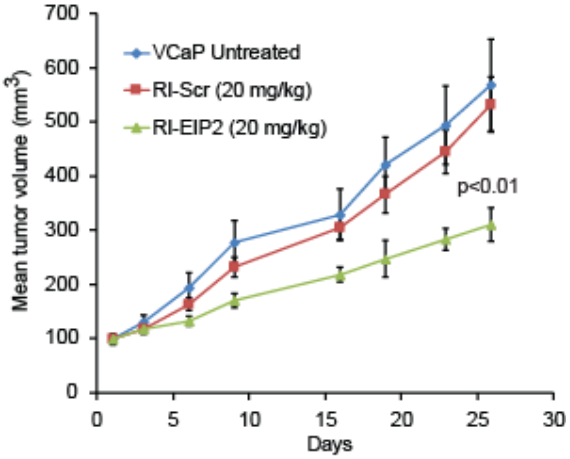
VCaP Untreated
RI-Scr (20 mg/kg)
RI-EIP2 (20 mg/kg)
p<0.01
Mean tumor volume (mm3)
Days

G

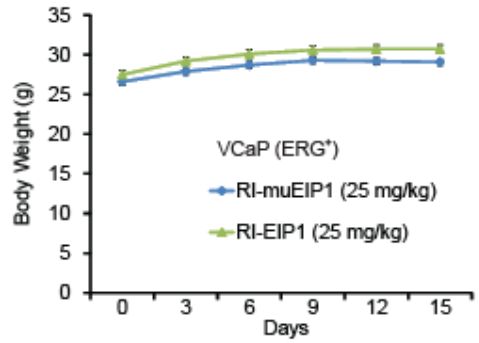
VCaP (ERG+)
RI-muEIP1 (25 mg/kg)
RI-EIP1 (25 mg/kg)
Body Weight (g)
Days

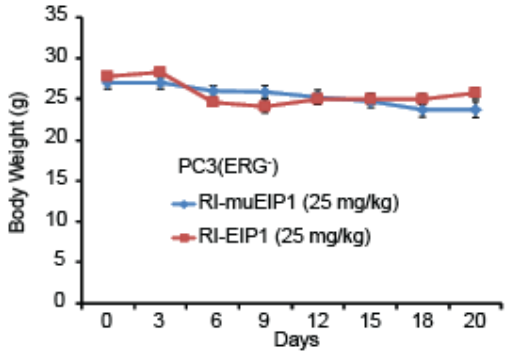
PC3(ERG-)
RI-muEIP1 (25 mg/kg)
RI-EIP1 (25 mg/kg)
Body Weight (g)
Days

H

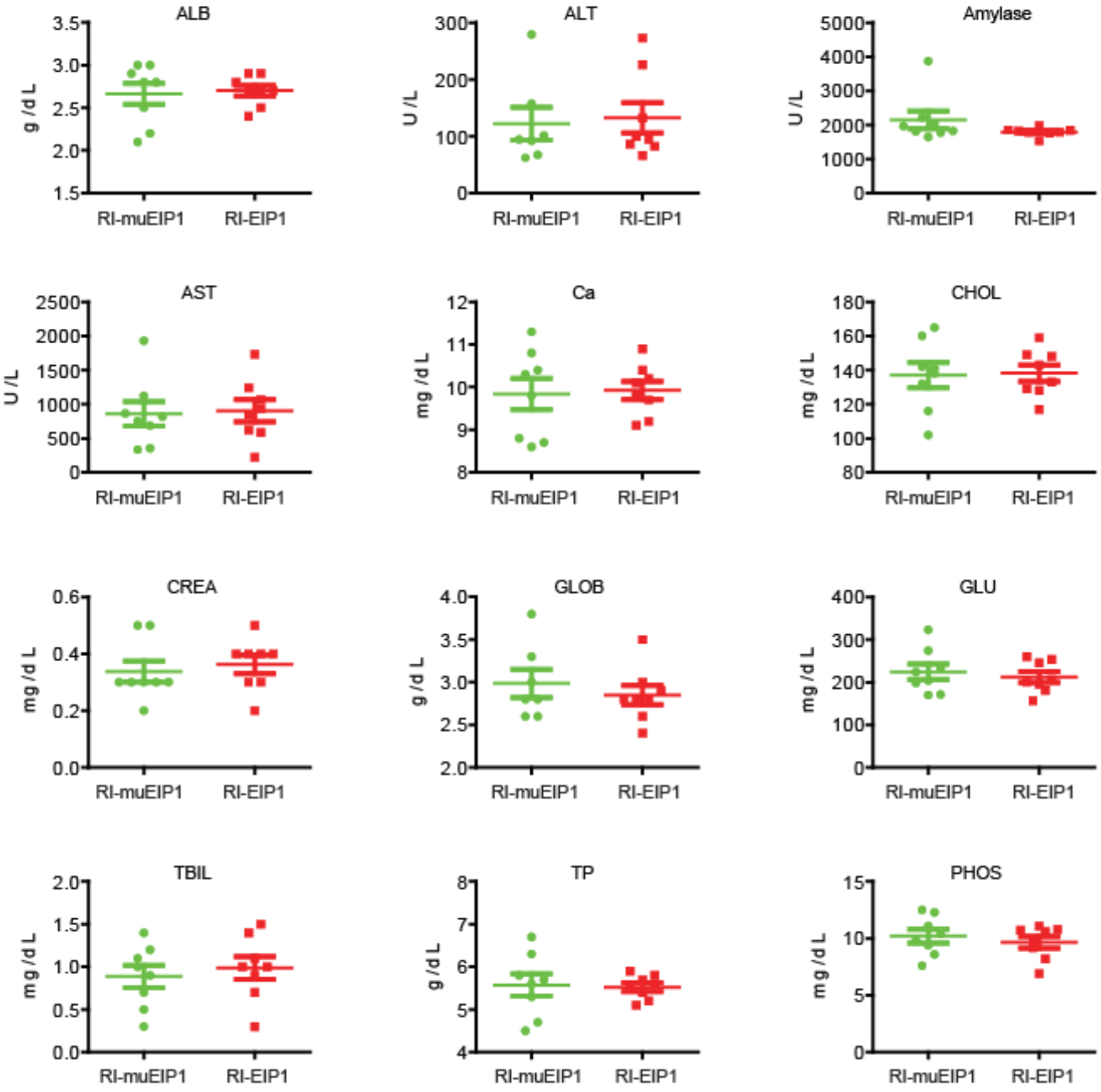
ALB
g /d L
3.5
3.0
2.5
2.0
1.5
RI-muEIP1
RI-EIP1
ALT
U /L
300
200
100
0
RI-muEIP1
RI-EIP1
Amylase
U /L
5000
4000
3000
2000
1000
0
RI-muEIP1
RI-EIP1
AST
U /L
2500
2000
1500
1000
500
0
RI-muEIP1
RI-EIP1
Ca
mg /d L
12
11
10
9
8
RI-muEIP1
RI-EIP1
CHOL
mg /d L
180
160
140
120
100
80
RI-muEIP1
RI-EIP1
CREA
mg /d L
0.6
0.4
0.2
0.0
RI-muEIP1
RI-EIP1
GLOB
g /d L
4.0
3.5
3.0
2.5
2.0
RI-muEIP1
RI-EIP1
GLU
mg /d L
400
300
200
100
0
RI-muEIP1
RI-EIP1
TBIL
mg /d L
2.0
1.5
1.0
0.5
0.0
RI-muEIP1
RI-EIP1
TP
g /d L
8
7
6
5
4
RI-muEIP1
RI-EIP1
PHOS
mg /d L
15
10
5
0
RI-muEIP1
RI-EIP1


I
367
375
ERG
RALRYYYDK
ETV1
RSLRYYYEK
J
Input
Biotin-muEIP1
Biotin-EIP1
Biotin-muEIP1
Biotin-EIP1
VCaP
LNCaP
αERG
αETV1
10 μM
50 μM

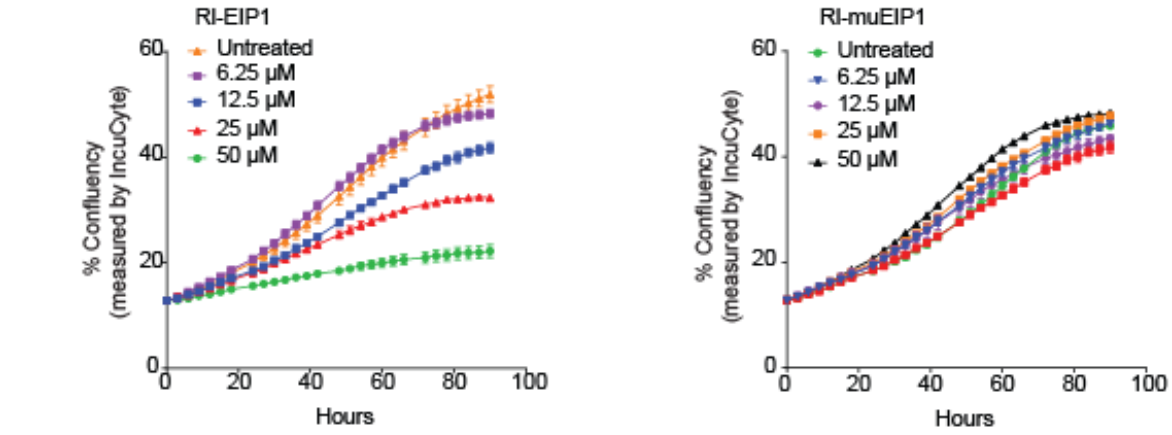
K
RI-EIP1
Untreated
6.25 μM
12.5 μM
25 μM
50 μM
% Confluency (measured by IncuCyte)
Hours
RI-muEIP1
Untreated
6.25 μM
12.5 μM
25 μM
50 μM
% Confluency (measured by IncuCyte)
Hours

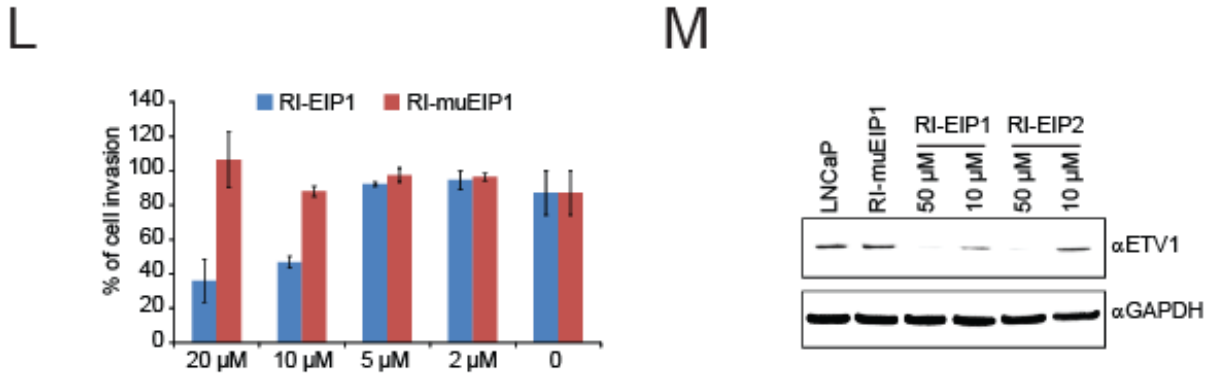
L
RI-EIP1
RI-muEIP1
% of cell invasion
20 μM
10 μM
5 μM
2 μM
0
M
LNCaP
RI-muEIP1
RI-EIP1
RI-EIP2
50 μM
10 μM
50 μM
10 μM
αETV1
αGAPDH

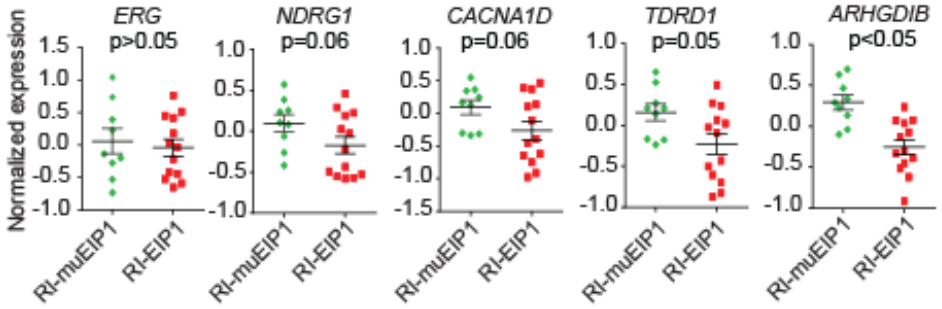
N
Normalized expression
ERG
p>0.05
NDRG1
p=0.06
CACNA1D
p=0.06
TDRD1
p=0.05
ARHGDIB
p<0.05
RI-muEIP1
RI-EIP1

Figure S7. Xenograft tumor response after treatment with the peptidomimetics, related to Figure 7.
(**A**) The serum concentration of biotinylated RI-EIP1 after intraperitoneal administration of 25 mg/kg in mice harboring VCaP xenografts was assessed by colorimetric assay (graph shows results from a representative sample). Serum was collected at indicated time points (x-axis) and the concentration of biotinylated peptides was determined by avidin-HRP reaction (y-axis).
(**B**) VCaP xenograft tumors treated with a single dose of 25 mg/kg RI-EIP1 were harvested at 3, 6, 18, 24 hours followed by IP-Western blot analysis with anti-DNA-PKcs antibody. ERG protein immunoprecipitated was also detected by an ERG antibody. Tumor lysates (1/100 input) were loaded as positive controls for DNA-PKcs, ERG and GAPDH.
(**C**) Immunoblot analysis of ERG and GAPDH in VCaP xenograft tumors treated with 25 mg/kg RI-EIP1 or RI-muEIP1 daily for 5 days. The tumors were collected at 7 days.
(**D**) Tumor volumes (in mm^3) for each VCaP-xenografted mice treated with RI-EIP1 or RI-muEIP1 for 18 consecutive days as in **Figure 7D**.
(**E**) VCaP-xenografted mice treated with RI-EIP1 or RI-muEIP1 for 24 consecutive days at various doses as indicated. Experiments were performed as **Figure 7D**.
(**F**) VCaP xenografted mice treated with RI-EIP2 or RI-Scr at indicated time points. Caliper measurements of average tumor volume (in mm^3) were recorded every three days. Experiments were performed as in **Figure 7D**.
(**G**) Body weight of mice after long-term treatment with RI-EIPs. Mice harboring VCaP or PC3 cell xenografts were weighed at the time of tumor volume measurements.
(**H**) Measurement of serum markers of toxicity in mice harboring xenografts treated for 24 consecutive days by either RI-EIP1 or RI-muEIP1.
(**I**) Sequence alignment of ERG and ETV1. The EIP interactive region from R^{367} to K^{375} is shown.
(**J**) Interaction of EIP with endogenous ETV1 protein expressed in LNCaP cells. Biotin-EIP1 or biotin-muEIP1 was incubated with LNCaP cell lysates. Eluates from the pull-downs were subjected to immunoblot analysis using anti-ETV1 antibody. VCaP cell lysates were used as positive control.
(K) Confluence rates for LNCaP cells were measured by IncuCyte; cells were treated with RI-EIP1 or RI-muEIP1 as indicated.
(**L**) Boyden chamber transwell invasion assays were performed in chambers pre-coated with Matrigel. Cells were pre-treated as indicated for 24 hours and allowed to invade for an additional 48 hours prior to fixation, imaging and quantification. The data represents the mean of three independent experiments.
(**M**) Immunoblot analysis of ETV1 and GAPDH from LNCaP cell treated with RI-EIP1/2 or RI-muEIP1 at indicated concentrations.
(**N**) Quantitative PCR was used to assess the relative expression of several ERG target genes in VCaP xenograft tumors in **Figure 7D**. The data shown represent the mean± SEM of triplicate experiments.